Dental Materials Journal 2010; 29(4): 438–445

Chemical analyses of hydroxyapatite formation on SAM surfaces modified with COOH, NH_2, CH_3, and OH functions

Isao HIRATA[1], Mai AKAMATSU[1], Eri FUJII[1], Suchit POOLTHONG[2] and Masayuki OKAZAKI[1]

[1]*Department of Biomaterials Science, Graduate School of Biomedical Sciences, Hiroshima University, 1-2-3 Kasumi, Minami-ku, Hiroshima 734-8553, Japan*
[2]*Department of Operative Dentistry, Faculty of Dentistry, Chulalongkorn University, Henri Dunant Rd, Bangkok 10330, Thailand*
Corresponding author, Masayuki OKAZAKI; E-mail: okazakix@hiroshima-u.ac.jp

Hydroxyapatite formation was examined at the surface of self-assembled monolayers (SAMs) modified with four functional groups, -COOH, -NH_2, -CH_3, and -OH. For COOH-SAM and NH_2-SAM, scanning electron spectroscopic observation showed that flake-like sheet crystals covered the whole wafer and small broccoli-like crystals were observed occasionally on the flake-like crystal base layer. For CH_3-SAM and OH-SAM, no flake-like sheet crystals were observed; broccoli-like crystals were observed in a dispersed manner for CH_3-SAM, but in localized spots for OH-SAM. X-ray diffraction patterns showed a strong apatite pattern oriented toward the c-axis direction for COOH-SAM. ESCA analysis revealed distinct Ca, P, O peaks for COOH-, NH_2-, CH_3-, and OH-SAM. Surface plasmon resonance (SPR) analysis indicated that during the supply of supersaturated calcium phosphate solution, the deposition of precipitates increased monotonically with time for COOH-SAM, increased slightly for NH_2-SAM, but little increase in deposition was detected for CH_3-SAM and OH-SAM.

Keywords: Hydroxyapatite formation, SAM surfaces, Surface plasmon resonance

INTRODUCTION

It is speculated that organic substances such as proteins play an important role at the initial stage of *in vivo* apatite formation. For example, collagen behaves as an extracellular matrix during bone formation[1)] and non-collagenous proteins such as gene proteins are present during enamel formation. The main functional groups of amino acids that construct proteins are -COOH, -NH_2, -CH_3, and -OH. It is interesting to note that these functional groups may be involved in initial apatite formation.

A self-assembled monolayer (SAM) is an organized layer of adjacent multiple linear organic molecules with a coupling agent at one end and a functionalized end group at the other, separated by an organic spacer. For research into the interfacial phenomena of bioadhesion and biocompatibility, SAMs have attracted significant attention because they provide a systematic way to modify the surface properties of materials such as gold wafers. To date, it has been reported that SAM surfaces on gold wafers could be modified with four typical functional groups, -COOH, -NH_2, -CH_3, and -OH, for apatite formation[2-4)].

Apart from the use of SAMs to produce biocompatible hydroxyapatite (HA) coatings on implant substrates, attention is also turned to biomaterials — such as titanium and its alloys or sintered ceramics— which possess the dual properties of good biocompatibility and strength. To expedite patient recovery, the need for implants to be rapidly osseointegrated led to the need for biomaterials with functionalized surfaces. Various techniques have been developed for producing HA coatings on implant surfaces, such as plasma spraying[5)], hot isostatic pressing (HIP)[6)], sol-gel technique and biomimetic precipitation[7)]. Unfortunately, subsequent heat treatment at high temperature results in cracking and poor bond strength between the hydroxyapatite coating and metal substrate. Further, an HA coating of high crystallinity, which is desirable for optimal biocompatibility, could not be achieved through these methods.

To improve the biological properties of HA coatings on biomaterials, several studies have explored and examined the approach of SAM-assisted HA coating of Ti implant surfaces. Liu *et al.*[8)] reported that HA formation was successfully achieved with -PO_4H_2 and -COOH, but not with -OH and -CH=CH_2. Notably, the -COOH end group appeared to provide the optimal SAM surface for nucleation and growth of biomimetic crystalline HA[8)]. This finding reinforced the notion that human bone sialoprotein is a potent nucleator of HA and is linked to the protein's glutamic acid-rich sequences. Therefore, the affinity for interaction between polar side groups on the protein and positive (calcium) or negative (phosphate) sites in the crystal is of significant interest. However, no detailed crystallographic and morphological studies of apatite formation on SAM surfaces have been reported.

Many researchers have used simulated body fluid (SBF) solutions in their investigations of apatite formation on functionalized surfaces[4,7-11)], but the reproducibility of data posed a problem. Moreover, in most investigations, SBF solutions were adapted to simulate clinical use, such as hydroxyapatite coating on titanium surface. In contrast, our focus was to obtain reproducible and stable results on the effects of

Received Feb 5, 2010: Accepted Apr 1, 2010
doi:10.4012/dmj.2010-017 JOI JST.JSTAGE/dmj/2010-017

different functional groups on hydroxyapatite formation. Therefore in this study, SAMs were modified with four functional groups, -COOH, -NH_2, -CH_3, and -OH[12-14], on gold wafer surfaces. Our next focus was to conduct a basic research on chemical analysis, where surface plasmon resonance (SPR) analysis —in addition to SEM, XRD, ESCA— was used for real-time observation of the early initial deposition of calcium phosphate. In view of this focus on chemical analysis, a simple CaP supersaturated solution was used in this study as opposed to an SBF containing Ca^{2+}, PO_4^{3-}, and OH^- ions with other trace elements, which was frequently used in experiments on biomimetic hydroxyapatite formation[4,7-11].

MATERIALS AND METHODS

Preparation of gold wafers

Glass plates (diameter: 15 mm, thickness: 1 mm) were supplied from Matsunami Glass Industries (Osaka, Japan). Gold wafers were prepared in Osaka Vacuum Industrial Co. Ltd. (Osaka, Japan) by first depositing Cr (1 nm) and then Au (49 nm) onto the glass plates under 2.0×10^{-2} Pa with electron beam heating.

Preparation of self-assembled monolayers (SAMs)

1-dodecanethiol (CH_3-SH) was purchased from Wako Pure Chemical Industries (Osaka, Japan). 11-mercapto-1-undecanol (OH-SH), 11-mercapto-1-undecanoic acid (COOH-SH), and 11-amino-1-undecanthiol (NH_2-SH) reagents were purchased from Sigma-Aldrich Japan (Tokyo, Japan).

The gold wafers were cleaned by immersion in a piranha solution (7:3 volume ratio of sulfuric acid and 30% H_2O_2) for 15 minutes and then washed three times with ultrapure water to remove contaminants. Following which, the gold wafers were immersed in ultrapure water until SAM deposition.

1 mmol/L COOH-SH, NH_2-SH, CH_3-SH and OH-SH solutions were prepared with nitrogen gas bubbled through deoxidized ethanol for 1 hour. The gold wafers were immersed in these alkanethiol solutions for 24 hours, and different kinds of SAMs (COOH-SAM, NH_2-SAM, CH_3-SAM, and OH-SAM) were formed independently on gold wafer surfaces (Fig. 1). These SAM wafers were immersed in 2-propanol until experiment was carried out.

Characterization of SAM surfaces

Surface chemical compositions of SAMs were determined using X-ray photoelectron spectroscopy (XPS or ESCA, AXIS-HS, Kratos, Manchester, UK) under 10^{-7} Pa. Monochromatic Al-Kα X-rays were used with a 15 kV acceleration voltage and 10 mA filament electric current. High-resolution spectra for carbon and oxygen elements were obtained at a takeoff angle of 35°.

Wettability of SAMs was measured beforehand using a lab-made static water contact angle measurement apparatus. For each water contact angle measurement, 0.5 μL of ultrapure water was dropped on each SAM —a measurement process which was repeated five times for each SAM. The mean contact angles of COOH-SAM, NH_2-SAM, CH_3-SAM, and OH-SAM were 14.1±4.1, 55.5±4.3, 104.4±2.8, and 4.6±1.6 degrees respectively (n=5).

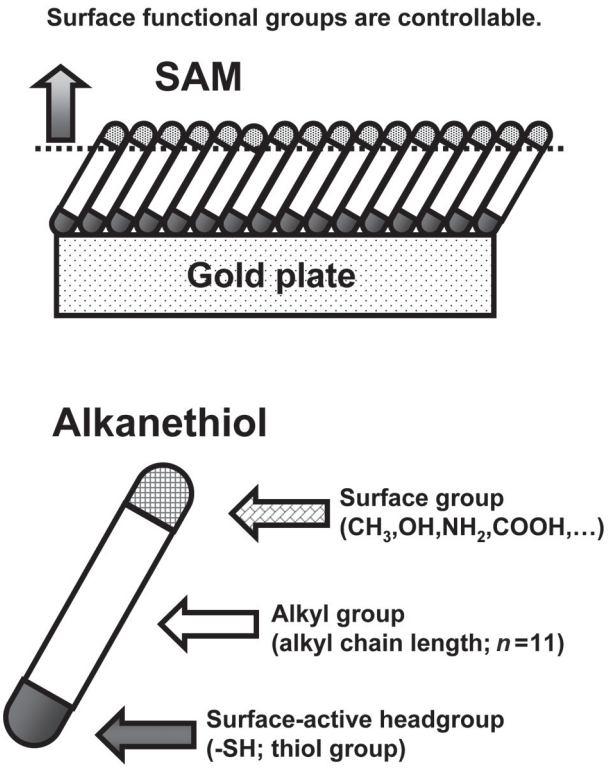

Fig. 1 Schema of a self-assembled monolayer (SAM).

SEM observation, XRD and ESCA analyses of precipitates on SAM surfaces

50 mmol/L $Ca(CH_3COOH)_2.H_2O$, 30 mmol/L $NH_4H_2PO_4$, and 1.3 mol/L CH_3COONH_4 were mixed at 1:1:2 to prepare a buffer solution of pH 7.4±0.2. Final calcium and phosphate concentrations in the mixed solution were 12.5 mmol/L and 7.5 mmol/L respectively. In a preliminary experiment, the solution of 12.5 mmol/L calcium and 7.5 mmol/L phosphate did not show observable precipitation for several hours after mixing, but slight precipitation after one-day incubation at 37°C. With a solution of 10.0 mmol/L calcium and 6.0 mmol/L phosphate, no precipitation was observed even after one-month incubation at 37°C. Therefore, in this study, the solution of Ca=12.5 mmol/L and P=7.5 mmol/L was adopted for the supersaturated calcium phosphate solution.

10 mL of the calcium phosphate solution was gently flowed into a plastic vessel, in which gold wafers coated with each SAM were set and incubated at 37°C (n=6). After 3 days and 1 week, SAM wafers were

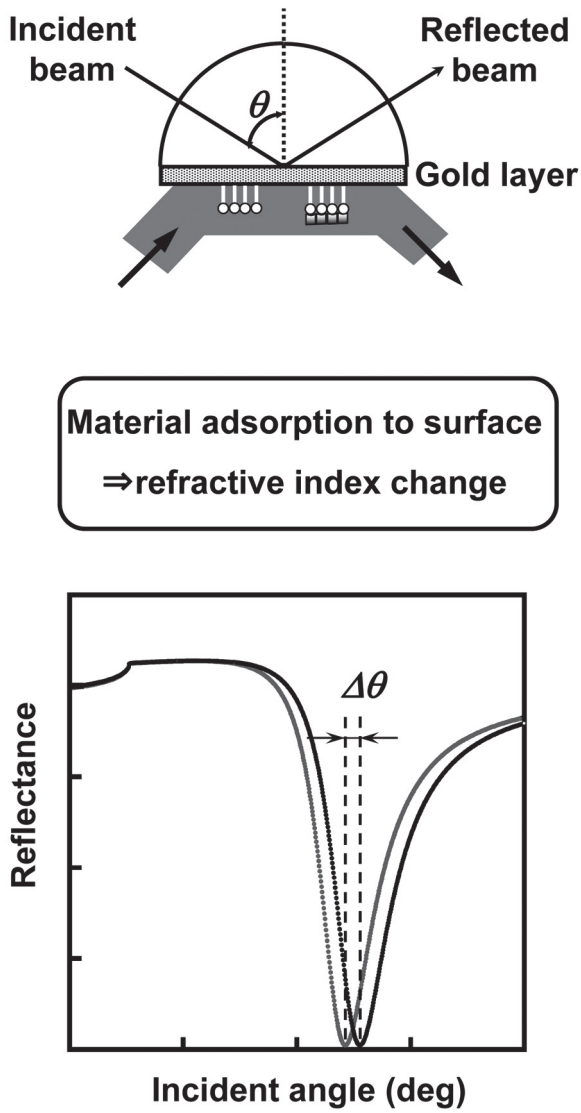

Fig. 2 Principle of surface plasmon resonance (SPR) detection.

rinsed with ultrapure water three times and then dried in a desiccator. After which, the SAM wafer surfaces were observed with a scanning electron microscope (SEM) and analyzed by X-ray diffraction (XRD) and electron spectroscopy for chemical analysis (ESCA).

SPR analysis of calcium phosphate deposition

In this study, amount of calcium phosphate deposition on each SAM was measured using a lab-made surface plasmon resonance (SPR) sensor. SPR is an optical technique for determining refractive index changes at a surface, which is typically an interface between a solid support phase and a liquid phase (Fig. 2).

A SAM wafer was set on the SPR flow stage. First, ultrapure water was injected and allowed to flow into the flow cell. At this juncture, a SPR reflectivity curve, which showed the intensity of the reflected light angle against the incidence angle, was recorded. Next, the same acetate buffer solution containing calcium phosphate described above was injected and allowed to flow into the cell for 15 minutes. Finally, the calcium phosphate solution was washed out of the flow cell with ultrapure water and the SPR reflectivity curve was recorded again. Amount of calcium phosphate deposited on each SAM was determined based on the SPR angle shift, which was defined as the angle difference between the minima of two SPR reflectivity curves. Medium flow was 2.5 mL/min and temperature was kept at 25ºC.

RESULTS

SEM observations of precipitates on SAM surfaces

After 3-day incubation, each wafer was washed three times and dried in a desiccator. COOH-SAM and NH_2-SAM surfaces were completely covered with a white precipitate, while CH_3-SAM was partially covered with a white precipitate. With OH-SAM, only a small amount of precipitate was observed on the wafer (Fig. 3: upper center).

For COOH-SAM and NH_2-SAM, SEM observation showed that flake-like sheet crystals covered the whole wafer and small broccoli-like crystals were observed occasionally on the flake-like crystal base layer (Figs. 3a and 3b). For CH_3-SAM and OH-SAM, no flake-like sheet crystals were observed and broccoli-like crystals were observed in a dispersed manner for CH_3-SAM (Fig. 3c). For OH-SAM, broccoli-like crystals were observed in localized spots (Fig. 3d). After 1-week incubation, there were no fundamental differences in the precipitate crystals formed on COOH-SAM (Fig. 4a). At high magnification, large plate-like crystals in the flake-like base layer were observed (Fig. 4b).

XRD analysis of precipitates on SAM surfaces

X-ray diffraction patterns showed a strong apatite pattern orientated toward the c-axis direction for COOH-SAM (Fig. 5a) and NH_2-SAM. For CH_3-SAM, no clear orientation of apatite was observed and peak intensity was weak (Fig. 5b). For OH-SAM, X-ray diffraction analysis was difficult because too few crystals were formed on the wafer surface.

ESCA analysis of precipitates on SAM surfaces

ESCA analysis revealed a strong O peak and distinct Ca and P peaks for COOH-, NH_2-, CH_3-, and OH-SAM (Fig. 6). For NH_2-SAM, an Au peak was observed probably because only a thin layer of hydroxyapatite was formed. For OH-SAM with only a small amount of precipitate formed on the wafer and a detected Au peak, ESCA analysis was still possible because ESCA analysis required only a limited micrometer area.

SPR analysis of calcium phosphate deposition on SAM surfaces

The SPR analysis shown in Fig. 7 indicated that the

deposition of precipitates increased with time monotonically for COOH-SAM during the supply of supersaturated calcium phosphate solution, increased slightly for NH_2-SAM, but increase in deposition was scarcely detected for CH_3-SAM and OH-SAM, probably because of lower affinity and short (15 minutes) supply of calcium phosphate solution.

DISCUSSION

SAM is a monolayer formed on the gold surface by inter-molecular attraction (Van der Waals forces)

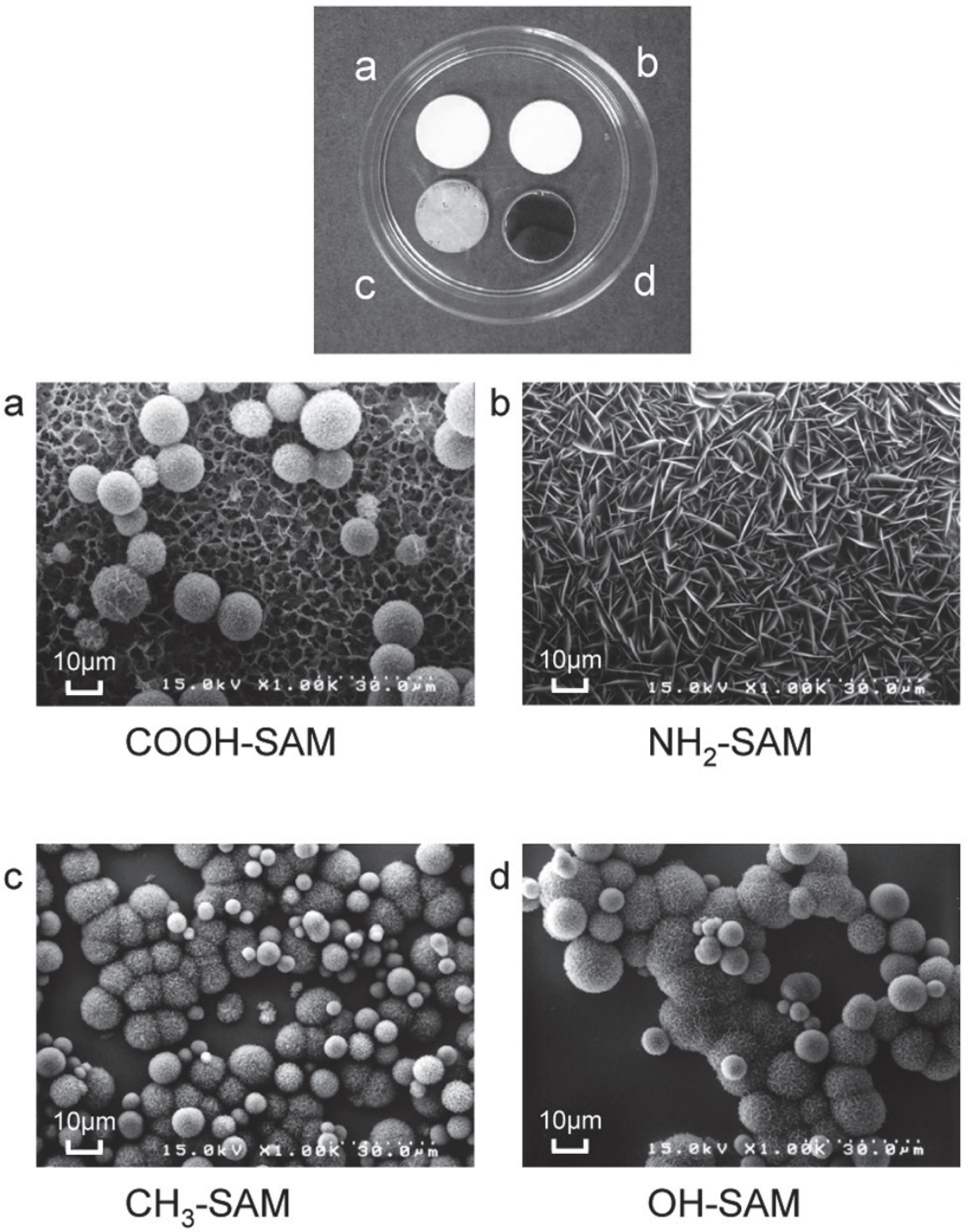

Fig. 3 Photo (upper center) and scanning electron micrographs (SEM) of the precipitates deposited on the surfaces of COOH-SAM (a), NH_2-SAM (b), CH_3-SAM (c), and OH-SAM (d) wafers after 3-day incubation at 37ºC.

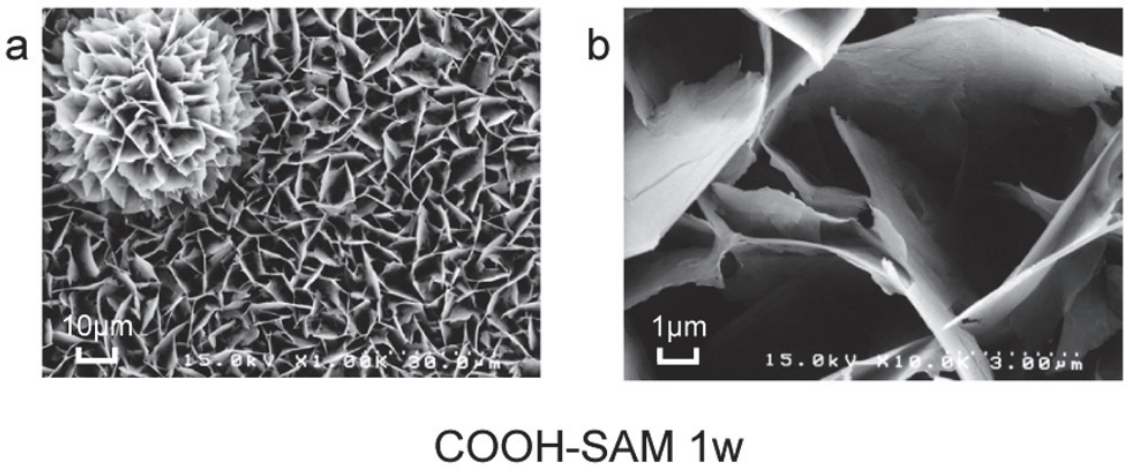

Fig. 4 Scanning electron micrographs (SEM) of the precipitates deposited on the surface of COOH-SAM after 1-week incubation at 37ºC (a) and the magnified photo of its flake-like base layer (b).

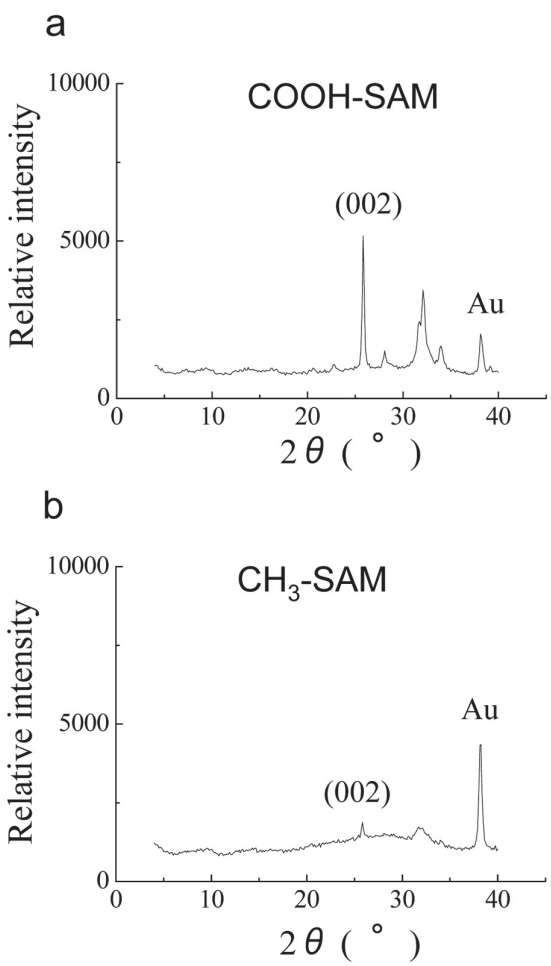

Fig. 5 X-ray diffraction (XRD) patterns of the precipitates deposited on the surface of COOH-SAM (a) and CH_3-SAM (b) wafer after 3-day incubation at 37ºC.

between a gold thiol head group and an alkyl chain group. Therefore, the physical adsorption of each functional group -COOH, -NH_2, -CH_3, and -OH on the gold wafer surfaces is caused by and controlled by Van der Waals force (Fig. 1). Results of this study then showed that the surface properties of SAM significantly affected the formation of calcium phosphate precipitates. Whereas adsorption was traditionally and typically explained using the concept of hydrophilic and hydrophobic phenomena, which are represented by -OH (water contact angle: 4.6 degree) and -CH_3 (water contact angle: 104.4 degree) functions respectively, this study revealed that there was low adsorption of calcium phosphate crystals on OH-SAM despite its very low water contact angle. On the other hand, COOH-SAM (water contact angle: 14.1 degree) and NH_2-SAM (water contact angle: 55.5 degree), which had an electrical charge, were favorable for apatite formation.

When discussing the wettability of a material's surface, chemical composition and especially electrical charge —in addition to surface roughness and morphology— must also be considered because interface affinity is very important. Since hydroxyapatite is an ionic crystal, the attraction —and adsorption— of positively charged calcium ions would promote apatite formation. As illustrated in Fig. 8, calcium ions are apt to be trapped by the double scissors of COO^- function to form a columnar Ca framework in hydroxyapatite (HAp) crystal. Subsequently, the hydroxyapatite crystals gradually oriented along the c-axis as shown in Fig. 5a.

In this study, the morphology of hydroxyapatite crystals dramatically changed according to the different functional groups, -COOH, -NH_2, -CH_3, and -OH, modified onto the SAM. For -COOH and -NH_2, large flake-like crystals were formed on the SAM surfaces. For -CH_3 and -OH, only small round crystals precipitated on the SAM surfaces. The morphological

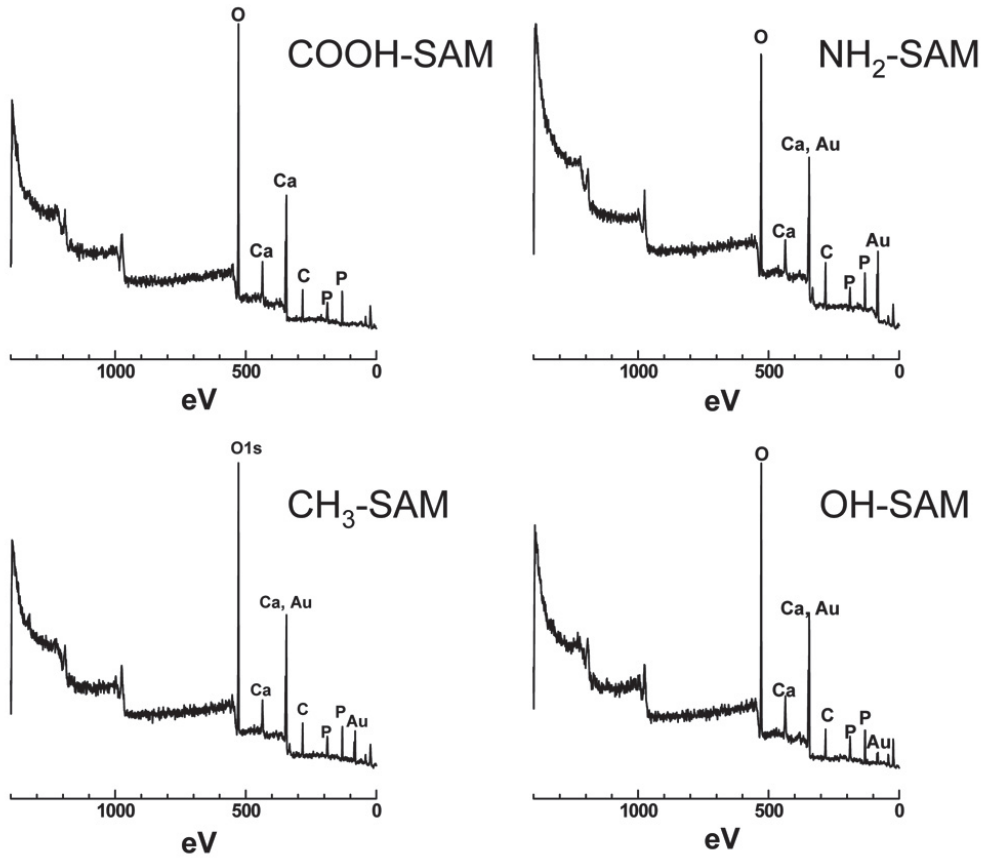

Fig. 6 Electron spectroscopy for chemical analysis (ESCA) spectra of the precipitates deposited on the surfaces of COOH-SAM, NH_2-SAM, CH_3-SAM, and OH-SAM wafers after 3-day incubation at 37ºC.

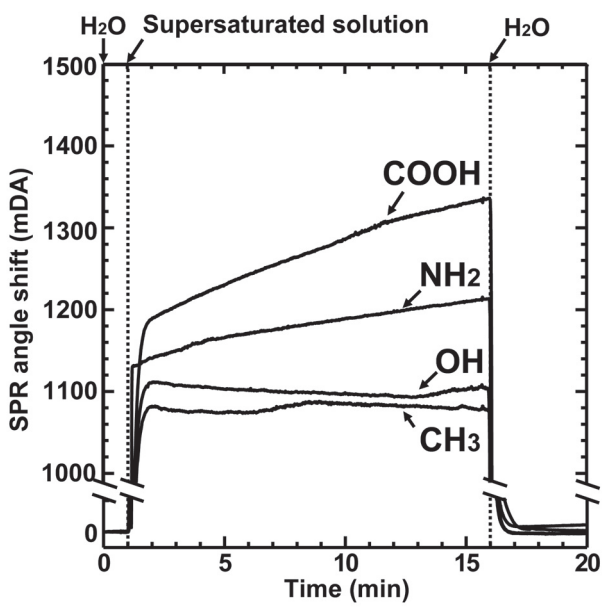

Fig. 7 SPR angle shifts as a function of real-time deposition on the surfaces of COOH-SAM, NH_2-SAM, CH_3-SAM, and OH-SAM wafers.

differences probably arose from the differences in electrical force attracting the calcium and phosphate ions, whereby the latter ions then initiated the formation of hydroxyapatite on SAM surfaces. In addition, it must be highlighted that the crystallinity and orientation reflected on the X-ray diffraction patterns (Fig. 6) are affected by crystal morphology, hence careful attention was paid to the experimental conditions in this study.

By using a simple calcium phosphate solution of a relatively higher concentration than SBF, stable and reproducible results were obtained in this study. On the quantitative assessment of apatite formation, SPR analysis was used in this study as opposed to the quartz crystal microbalance (QCM) which was used in previous studies[9-11]. The QCM detects weight gain on the charged surfaces, but is strongly affected by small changes in temperature, viscosity, and/or hydrodynamic conditions. On the contrary, SPR uses laser light to detect angle changes on a material surface until a stable SPR angle signal is attained and is less affected by the aforementioned conditions. Therefore, compared to QCM, SPR is capable of analyzing molecular-level surfaces and is hence more suitable for detecting the initial stage of apatite formation.

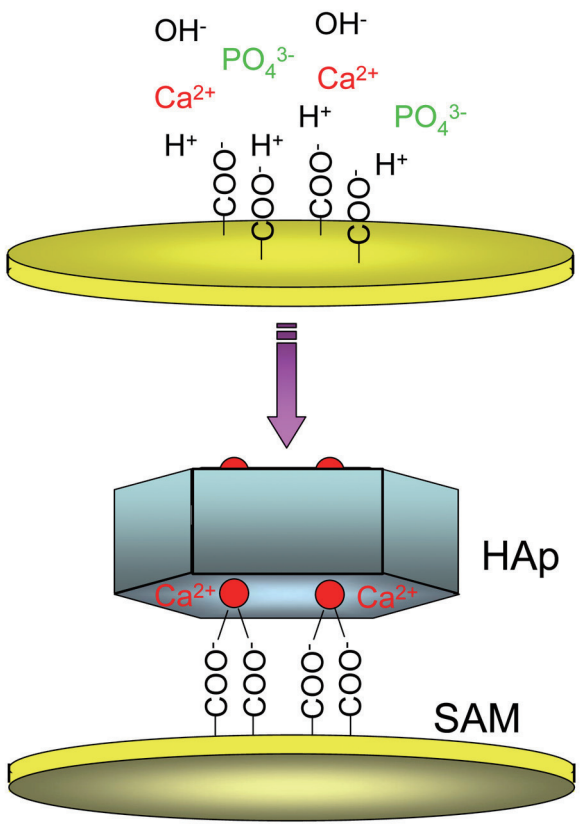

Fig. 8 Schematic model of initial hydroxyapatite (HAp) crystal formation on COOH-SAM surface.

SPR is commonly used for nanometer-scale detection of protein-protein interactions, molecular adsorption, and surface structure changes, using an He-Ne laser light, Knoll's method[15], and a Kretschmann configuration[16]. General SPR sensor chips are produced by depositing gold on a glass surface with an ultrathin layer of chromium or titanium as a binding material. With the use of SPR in this study, calcium phosphate formation was successfully observed in real-time. Precipitate deposition results seemed to suggest that the calcium phosphate formed might be hydroxyapatite, although a direct identification was difficult because of real-time deposition during SPR analysis and an extremely small amount of deposition. At the same time, however, the SPR angle (mDA) for COOH-SAM shown in Fig. 7 enabled the thickness of the precipitate layer to be estimated to be 0.71 nm. This was because the SPR angle shift was 352 mDA/nm, and the net value of angle shift for COOH-SAM was read as 250 mDA from the data in Fig. 7. This value was close to the c-axis unit dimension of hydroxyapatite, which was 0.688 nm. In other words, it was suggested that during the 15-minute supply of calcium phosphate solution, a monolayer of amorphous calcium phosphate approximately equal to the c-axis unit dimension of hydroxyapatite was formed.

Another important factor that influences calcium phosphate formation is the pH condition. Hydroxyapatite (HAp) forms in alkaline conditions; in strongly acidic conditions, it is mainly dicalcium phosphate dehydrate (DCPD)[17]; and in weakly acidic conditions near pH 7.0, it could be tricalcium phosphate (TCP)[18] and octacalcium phosphate (OCP)[19]. In the present study, an acetate buffer solution of pH 7.4 was used. Therefore, the deposited calcium phosphate would transform to hydroxyapatite if the experiment were to continue for a longer period. Nonetheless, it must be put into perspective that the deposition obtained during this short 15-minute SPR experiment was estimated as a single unit layer, and coupled with a very low experimental temperature at 25°C, it was difficult to clearly identify the deposited crystal as hydroxyapatite. This is because apart from the pH condition, the morphology of calcium phosphate crystals is also significantly affected by the temperature and co-existing trace elements in the solution.

CONCLUSION

The -COOH, -NH_2, -CH_3, and -OH functional groups of proteins exhibited different behaviors in terms of hydroxyapatite formation. -COOH and -NH_2 functions were favorable for hydroxyapatite formation when compared with -OH and -CH_3. These results would be useful toward the design and development of novel functionalized biomaterials. SPR analysis was also found to be very useful for real-time observation of nanoscale calcium phosphate deposition, and the results obtained positively complemented with those of SEM, XRD, and ESCA.

ACKNOWLEDGMENTS

This study was supported in part by a Grant-in-aid for Scientific Research, No. 18390515, from the Ministry of Education, Science, Sports and Culture of Japan.

REFERENCES

1) Alberts B, Bray D, Lewis J, Raff M, Roberts K, Watson JD. Molecular biology of the cell, 3rd ed. New York: Garland Publishing; 1994. p. 1182-1186.
2) Campbell AA, Fryxell GE, Linehan JC, Graff GL. Surface-induced mineralization: a new method for producing calcium phosphate coatings. J Biomed Mater Res 1996; 32: 111-118.
3) Liu Q, Ding J, Mante FK, Wunder SL, Baran GR. The role of surface functional groups in calcium phosphate nucleation on titanium foil: a self-assembled monolayer technique. Biomaterials 2002; 23: 3103-3111.
4) Tanahashi M, Matsuda T. Surface functional group dependence on apatite formation on self-assembled monolayers in a simulated body fluid. J Biomed Mater Res 1997; 34: 305-315.
5) Yan L, Leng Y, Weng LT. Characterization of chemical inhomogeneity in plasma-sprayed hydroxyapatite coatings. Biomaterials 2003; 24: 2585-2592.
6) Hero H, Wie H, Jorgensen RB. Hydroxyapatite coatings on

Ti produced by hot isostatic pressing. J Biomed Mater Res 1994; 28: 343-348.
7) Kokubo T, Kusitani H, Sakka S, Kitsugi T, Yamamuro T. Solutions able to reproduce *in vivo* surface structure changes in bioactive glass-ceramic. Biomaterials 1990; 24: 721-734.
8) Liu DP, Majewski P, O'Neill BK, Ngothai Y, Colby CB. The optimal SAM surface functional group for producing a biomimetic HA coating on Ti. J Biomed Mater Res A 2006; 77: 763-772.
9) Zhu PX, Masuda Y, Koumoto K. Site-selective adhesion of hydroxyapatite microparticles on charged surfaces in a supersaturated solution. J Colloid and Interface Sci 2001; 243: 31-36.
10) Zhu PX, Masuda Y, Yonezawa T, Koumoto K. Investigation of apatite deposition onto charged surfaces in aqueous solutions using a quartz-crystal microbalance. J Am Ceram Soc 2003; 86: 782-790.
11) Zhu PX, Masuda Y, Koumoto K. The effect of surface charge on hydroxyapatite nucleation. Biomaterials 2004; 25: 3915-3921.
12) Hirata I, Hioki Y, Toda M, Kitazawa T, Murakami Y, Kitano E, Kitamura H, Ikada Y, Iwata H. Deposition of complement protein, C3b, on mixed self-assembled monolayers carrying surface hydroxyl and methyl groups studied by surface plasmon resonance. J Biomed Mater Res A 2003; 66: 669-676.
13) Hirata I, Morimoto Y, Murakami Y, Iwata H, Kitano E, Kitamura H, Ikada Y. Study of complement activation on well-defined surfaces using surface plasmon resonance. Colloids Surf B Biointerfaces 2000; 18: 285-292.
14) Fuse Y, Hirata I, Kurihara H, Okazaki M. Cell adhesion and proliferation patterns on mixed self-assembled monolayers carrying various ratios of hydroxyl and methyl groups. Dent Mater J 2007; 26: 814-819.
15) Knoll W. Polymer thin films and interfaces characterized with evanescent light. Makromol Chem 1991; 192: 2827-2856.
16) Kretschmann E. Determination of the optical constants of metals by excitation of surface plasma. Z Phys 1971; 241: 313-324.
17) Brown WE, Patel PR, Chow LC. Formation of $CaHPO_4.2H_2O$ from enamel mineral and its relationship to caries mechanism. J Dent Res 1975; 54: 475-481.
18) Termine JD, Posner AS. Amorphous crystalline interrelationship in bone mineral. Calcif Tiss Res 1967; 1: 8-23.
19) Brown WE. Crystal growth of bone mineral. Clin Orthop 1966; 44: 205-220.